Optimal Lane-Free Crossing of CAVs Through Intersections

Mahdi Amouzadi, Mobolaji Olawumi Orisatoki, and Arash M. Dizqah, *Member, IEEE*

***Abstract*—Connected and autonomous vehicles (CAVs), unlike conventional cars, will utilise the whole space of intersections and cross in a lane-free order. This article formulates such a lane-free crossing of intersections as a multi-objective optimal control problem (OCP) that minimises the overall crossing time, as well as the energy consumption due to the acceleration of CAVs. The constraints that avoid collision of vehicles with each other and with road boundaries are smoothed by applying the dual problem theory of convex optimisation. The developed algorithm is capable of finding the lower boundary of the crossing time of a junction which can be used as a benchmark for comparing other intersection crossing algorithms. Simulation results show that the lane-free crossing time is better by an average of 40% as compared to the state-of-the-art reservation-based method, whilst consuming the same amount of energy. Furthermore, it is shown that the lane-free crossing time through intersections is fixed to a constant value regardless of the number of CAVs.**

***Index Terms*—Connected and autonomous vehicles, dual problem theory, path planning, signal-free intersection.**

I. Introduction

INTERSECTIONS with traffic lights are inefficiently scheduled due to the limitations of human drivers which results in major congestion in urban traffic systems. Intersections also account for a large portion of all accidents (e.g. 47% in the United State in 2010 [1]). CAVs will be able to execute more complex manoeuvres than human drivers to cross intersections faster and safer, that also reduces energy consumption and increases traffic throughput [2]. However, these potential improvements require addressing three main challenges: collision avoidance, finding the minimum-time optimal solution instead of only checking the feasibility, and real-time implementation. Table I provides a summary of challenges and the corresponding techniques.

Previous studies proposed three approaches to ensure collision avoidance among CAVs:

i) Reserving the whole intersection for one of the CAVs at a time; The authors in [3] designed an algorithm based on solving an OCP that jointly improves energy consumption and passenger comfort. The proposed OCP includes collision avoidance constraints that enforce CAVs to reserve the whole intersection for a period of time. A similar work is presented by Tallapragada et al. in [4], where CAVs are split into clusters and each cluster reserves the whole area of the intersection for some time. The authors in [5], [6] introduced a scheduling method where CAVs are placed into a virtual lane based on their distance to the centre of the intersection and their risk of collision. Then, crossing time of the intersection is scheduled between the CAVs in the virtual lane. The study in [7] also proposes an algorithm for CAVs based on the concept of reserving the whole intersection for one CAV at a time. It is shown that the proposed algorithm reduces the mean fuel consumption of every vehicle by 13.29-73.11% as compared to traffic lights [7].

ii) Reserving a finite number of specific points (called conflict points) instead of the whole of the intersection; Mirheli et al. [8], [9] designed 16 conflict points for a four-leg intersection. Each leg of the intersection includes exclusively left turn and straight lanes. The proposed algorithm enforces CAVs to reserve the approaching conflict point(s) prior to their arrival. A more recent study of the conflict-point-reservation technique is presented in [10] where CAVs are capable of performing turning maneuvers. The algorithm initially finds the passing sequence of CAVs and then calculates the optimal control inputs analytically. The authors compared the energy consumption of CAVs when the algorithm finds the passing sequence using different strategies. It is shown that the best performance in terms of fuel consumption and travelling time is achieved when the passing sequence of CAVs is solved using the Monte Carlo Tree Search [10].

Another conflict point reservation approach is presented in [11] which allows flexible lane direction (e.g., incoming vehicles can travel to any outgoing lanes). In this work, a formation reconfiguration method is utilised to control longitudinal and lateral position of vehicles while avoiding collisions by reserving the conflict points. It is shown that crossing intersections with flexible lane direction technique outperforms signalised intersections and unsignalised intersections with fixed lane direction in terms of traffic throughput. A similar work is provided in [12] that designs an intersection crossing algorithm with a focus on erasing lane changes. This work also avoids collisions by reserving the conflict points through solving an optimisation problem that yields the optimal collision-free arriving times to the conflict points.

iii) Utilising the whole space of intersections freely, a.k.a. lane-free crossing; Generally speaking, reservation-based collision avoidance approaches require CAVs following predefined paths and not fully exploiting the intersection area. These types

Manuscript received 12 March 2022; revised 11 June 2022 and 8 August 2022; accepted 3 September 2022. Date of publication 15 September 2022; date of current version 13 February 2023. The review of this article was coordinated by Dr. Bo Yu. *(Corresponding author: Mahdi Amouzadi.)*

The authors are with the School of Engineering and Informatics. Smart Vehicles Control Laboratory (SVeCLab), University of Sussex, Brighton BN1 9RH, U.K. (e-mail: m.amouzadi@sussex.ac.uk; m.orisatoki@sussex.ac.uk; a.m.dizqah@sussex.ac.uk).

Digital Object Identifier 10.1109/TVT.2022.3207054

TABLE I
SUMMARY OF THE CHALLENGES OF THE INTERSECTION CROSSING PROBLEM AND THE CORRESPONDING TECHNIQUES FOR THE CHALLENGES

Challenge	Techniques to address	Implemented in
Collision avoidance	Reservation of the whole Intersection	[4, 5, 13, 3, 6, 7]
	Reservation of conflict points	[8, 14, 9, 11, 12]
	Lane-free	[15, 16]
Finding the minimum-time optimal solution instead of only checking the feasibility	Minimisation of fluctuation of the vehicles' acceleration	[16, 4]
	Minimisation of deviation from the speed limit	[17, 18, 19, 20]
	Minimisation of the crossing time	[15]
Real-Time implementation	Centralised strategies with fully-observable data	[15, 16, 18, 19]
	Decentralised strategies with fully connected CAVs	[21, 22]
	Decentralised strategies with partially connected CAVs	[23, 6]

of collision avoidance approaches are not efficient in terms of reducing travelling time and energy consumption. Prior studies developed lane-free algorithms based on OCP in [15], [16]. To avoid collisions, the Euclidean distance between any pair of CAVs are constrained to be greater than a safe margin. This formulation of the collision avoidance constraints is non-convex, and hence any optimisation problem including them are difficult to solve. Li et al. in [15] divided the non-differentiable and non-convex problem of intersection crossing into two stages to make it tractable. At stage one, CAVs inform the central controller with their intention and then make a standard formation which is computed online. At stage two, the controller searches an offline constructed lookup table for the intended crossing scenario and finds the control inputs of each CAV. The authors suggested to solve offline an individual optimal control problem for any possible crossing scenario to construct the lookup table of the control commands. However, the resulting offline problems are still non-differentiable and solving them for all possible scenarios of 24 CAVs take around 358 years [15]. Alternatively, Li et al. in [16] fixed the crossing time to a constant value and converted the minimum-time optimal control problem to a feasibility one to solve online.

As the second challenge, the above-mentioned algorithms that only find a feasible (collision-free) solution to the problem of the intersection crossing do not fully exploit the CAVs' advantages to minimise the crossing time. In other words, minimising the crossing time is not part of their objectives. The studies carried out in [4] and [16] focus on the passenger comfort and addressed the challenge by minimising fluctuation of the vehicles' acceleration. Other researchers in [17], [18], [19], [20] optimised the motion of CAVs to move on the predefined paths, reserving conflict points, with as close speed as possible to the limit of the intersection rather than directly finding the minimum-time paths. However, in complex scenarios, these paths need to be obtained as the solution of a minimum-time OCP instead of heuristically. The authors in [15] formulate the intersection crossing problem of CAVs as a minimum-time OCP to minimise the crossing time without any restrictions on the crossing paths (except the road boundaries). However, their algorithm is not time-effective for real-time applications.

Finally, it is always challenging to implement optimal control strategies in real-time. CAVs are intelligent agents communicating to each other and to the infrastructure to share information such as location, speed, and intentions. The optimal strategies for crossing intersections, therefore, must operate on a network of cars (i.e., networked controller), considering the shared information to control multiple CAVs which are seeking conflicting objectives (like minimising their individual crossing times). A centralised topology with a fully available information of all the CAVs or different decentralised topologies, where the CAVs are fully or partially connected, can be used to calculate the optimal crossing strategy of all the CAVs. The centralised controllers receive information of all vehicles, compute trajectories, and send back the calculated trajectory of each individual CAV. There is no path planning at the CAV level and vehicles only follow the provided trajectories. Li et al. [15], [16] proposed a centralised, but computationally expensive, optimal controller for multiple CAVs crossing a lane-free intersection. The centralised algorithms in [18], [19] split the problem into two stages, finding the crossing order and calculating the control inputs to follow the attained crossing orders, to make it computationally tractable.

In the decentralised strategies, on the other hand, each CAV computes its own trajectory by solving or approximating the solution of an optimal control problem to achieve a level of both the local and global objectives. The authors in [21], [22] formulated a decentralised OCP controller of the CAVs crossing intersections where each CAV has access to the shared information of all the others. Although decentralised algorithms find sub-optimal solutions, it is shown to be less computationally expensive as compared to the centralised counterparts [21], [22].

However, the CAVs which are crossing an intersection cannot be practically fully connected to each other at all the times. This means that at any instance of time, each CAV only communicates with a subset of the others, i.e. partially connected. Bian et al. [23] proposed a framework where the CAVs travelling on the same lane can communicate to each other, but they estimate the states of the other not-connected vehicles. Reference [6] proposes a partially connected distributed algorithm based on the concept of virtual platooning. CAVs, first, form a virtual platoon and then optimise their arriving time to the intersection to avoid collision. This is a decentralised reservation-based algorithm that allows only one CAV at a time within the intersection. Generally speaking, unlike the centralised controllers which are capable of finding the global optimum solution, decentralised controllers can only find sub-optimal strategies [24].

In summary, majority of the literature propose reservation-based algorithms which calculate the feasible collision-free trajectory. To the best of the authors' knowledge, there is a limited number of literature dealing with lane-free minimum-time crossing of intersections. In addition, there is no analysis and comparison of lane-free intersections in terms of crossing time, energy consumption and passenger comfort. The lane-free minimum-time crossing is a non-differentiable and non-convex NP-hard problem which are difficult to be solved with the state-of-the-art gradient-based algorithms. This paper addresses these gaps by the following novel contributions:

- Formulation of the lane-free crossing of CAVs through signal-free intersections as a minimum-time OCP;
- Smoothing of the constraints that avoid collisions of CAVs with each other and with road boundaries using the dual problem theory of convex optimisation. The constraints are also relaxed with sufficient conditions to make them computationally inexpensive;
- Minimisation of the crossing time of multiple CAVs passing through intersections in a lane-free order. It is shown that the minimum crossing time calculated by the proposed algorithm is very close to its theoretical limit. The calculated optimal crossing time for a junction is fixed to a constant value regardless of the number of CAVs until reaching the maximum temporal-spatial capacity of the intersection;
- Analysis and comparison of crossing time, energy consumption (due to acceleration) and passenger comfort of the proposed lane-free algorithm against a reservation-based method and a lane-free method. It is shown that the proposed lane-free algorithm significantly improves the crossing time and passenger comfort while consuming the same amount of energy as both the benchmark methods.

The remainder of this paper is organised as follows: Section II describes the system of multiple CAVs crossing an intersection and presents the notations used throughout the paper; Section III formulates the lane-free crossing of CAVs through an intersection as a minimum-time optimal control problem; Section IV provides numerical results obtained from simulation along with discussions, and Section V concludes the outcomes.

II. System Description

A. Lane-Free and Signal-Free Intersections

Fig. 1 illustrates an example layout of a lane-free and signal-free intersection. The figure includes three CAVs which are moving from their initial points, depicted with the most solid colour, towards their intended destinations which are with the most transparent colour. The intersection comprises of four approaches, each of them has a separate incoming and outgoing lane. In a lane-free intersection, vehicles can freely change their lanes in favour of faster crossing through the intersection. For instance, Fig. 1 shows the green CAV overtakes the black CAV by using the opposite lane.

In this study, the intersection does not have traffic lights because the CAVs can directly communicate their states and intentions. There is a coordinator that receives all the information

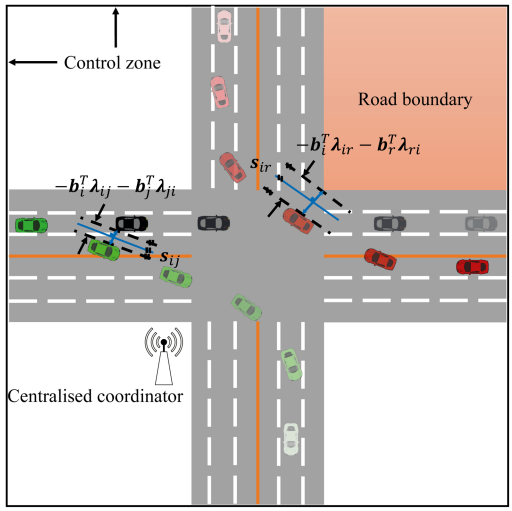

Fig. 1. Layout of the studied lane-free and signal-free intersection which also shows the sufficient conditions for obstacle avoidance. Further details are presented in section III.

from the CAVs when they arrive to the control zone and centrally control them to efficiently and safely cross the intersection. The control zone is defined based on the communication range of the coordinator, that is assumed 50 m. The coordinator then counts the number of vehicles entering the zone and when the number of vehicles reaches its practical limit or one of the vehicles reaches the beginning of the intersection, the coordinator calculates a safe trajectory for all the vehicles within its range. There is no human-driven vehicle or pedestrian. To compare the results with the ones of the prior research, this paper assumes that CAVs drive within the lanes before and after the control zone, which is shown to have no effects on the provided results (the results depend on the longest path of travelling CAVs). The authors in [25], [26], on the other hand, suggest that CAVs will drive in a seamlessly lane-free order within and outside intersections. In other words, there will not be a separate controller for different sections of roads and CAVs continuously collaborate to reach their final destinations without collision.

In Fig. 1, the black and green CAVs also show the collision avoidance. In this regard, the expression $-\mathbf{b}_i^\top\boldsymbol{\lambda}_{ij} - \mathbf{b}_j^\top\boldsymbol{\lambda}_{ji}$ is the dual representation of the distance between a pair of CAVs, and $\boldsymbol{s}_{ij}$ is the separating hyperplane placed between them. The parameters $\mathbf{b}_i$ and $\mathbf{b}_j$ are related to the size of CAV$_i$ and CAV$_j$ respectively and $\boldsymbol{\lambda}_{ij}$, $\boldsymbol{\lambda}_{ji}$ and $\mathbf{s}_{ij}$ are dual variables. Similarly, the red CAV and the highlighted road boundary show the road boundary avoidance. $-\mathbf{b}_i^\top\boldsymbol{\lambda}_{ir} - \mathbf{b}_r^\top\boldsymbol{\lambda}_{ri}$ is the dual representation of distance between a CAV and a road boundary and $\mathbf{s}_{ir}$ is the separating hyperplane between them. $\mathbf{b}_r$ is related to the size of the road boundary and $\boldsymbol{\lambda}_{ir}$, $\boldsymbol{\lambda}_{ri}$ and $\mathbf{s}_{ir}$ are the dual variables. For further details, the reader is referred to III-A and III-B.

B. Vehicle Kinematics

This study represents the lateral behaviour of CAVs with the bicycle model [27]. The bicycle model consists of two degree-of-freedom (DoF) which are sideslip angle β_i and yaw rate r_i,

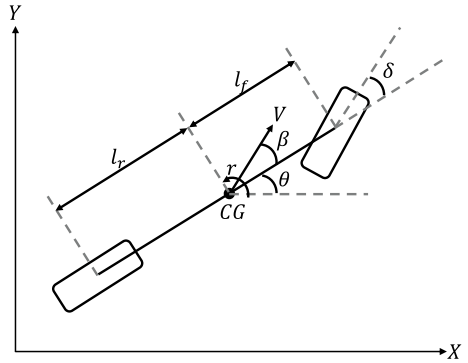

(a)

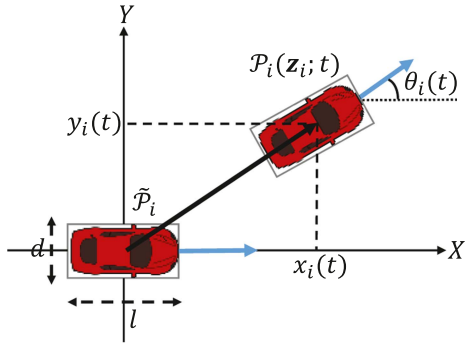

(b)

Fig. 2. (a) The bicycle model of vehicles. (b) Transformation of each CAV$_i$ from $\tilde{\mathcal{P}}_i$ to $\mathcal{P}_i(\mathbf{z}_i;t)$ where $\mathbf{z}_i(t)=[x_i(t),y_i(t),\theta_i(t)]^T$.

as in Fig. 2(a). The model also includes an additional DoF for the longitudinal velocity V_i. The equations of these DoFs along with other three to model the ground-fixed location, construct a set of differential equations to represent CAV$_i$ as follows:

$$\frac{d}{dt}\begin{bmatrix} r_i \\ \beta_i \\ V_i \\ x_i \\ y_i \\ \theta_i \end{bmatrix}(t) = \begin{bmatrix} \frac{\tilde{N}_r}{I_z\cdot V_i(t)}\cdot r_i(t) + \frac{N_\beta}{I_z}\cdot\beta_i(t) \\ \left(\frac{\tilde{Y}_r}{m\cdot V_i(t)^2}-1\right)\cdot r_i(t) + \frac{Y_\beta}{m\cdot V_i(t)}\cdot\beta_i(t) \\ 0 \\ V_i(t)\cdot cos\theta_i(t) \\ V_i(t)\cdot sin\theta_i(t) \\ r_i(t) \end{bmatrix} + \begin{bmatrix} 0 & \frac{N_\delta}{I_z} \\ 0 & \frac{Y_\delta}{m\cdot V_i(t)} \\ 1 & 0 \\ 0 & 0 \\ 0 & 0 \\ 0 & 0 \end{bmatrix}\begin{bmatrix} a_i \\ \delta_i \end{bmatrix}(t), t\in[t_0,t_f]\,. \quad (1)$$

where $[r_i,\beta_i,V_i,x_i,y_i,\theta_i]^T$ and $[a_i,\delta_i]^T$ are, respectively, the system states and control inputs of CAV$_i$. $\mathbf{z}_i=[x_i,y_i,\theta_i]^T$ refers to the pose of CAV$_i$ in non-inertial reference system. $a_i(t)$ and $\delta_i(t)$ are, respectively, the acceleration (m/s^2) and steering angle (rad) of the vehicle. The constants m and I_z denote mass (kg) and moment of inertia $(kg.m^2)$ of the vehicle. t_0 and t_f represent the starting and final time (s) of crossing the intersection. The vehicle parameters $\tilde{N}_r$, N_β, N_δ, $\tilde{Y}_r$, Y_β and Y_δ are calculated as follows [27]:

$$\begin{aligned} \tilde{N}_r &= l_f^2\cdot C_F + l_r^2\cdot C_R, \\ N_\beta &= l_f\cdot C_F - l_r\cdot C_R, \\ N_\delta &= -l_f\cdot C_F, \\ \tilde{Y}_r &= l_f\cdot C_F - l_r\cdot C_R, \\ Y_\beta &= C_F + C_R, \\ Y_\delta &= -C_F. \end{aligned}$$

where C_F and C_R are, respectively, the cornering stiffness of the front and rear tyres. l_f and l_r are distance of the front and rear axis from center of gravity of the vehicle.

To ensure CAVs drive within their dynamic limitations, the following constraints are enforced for each CAV$_i$:

$$\underline{V} \le V_i(t) \le \bar{V}, \quad (2a)$$
$$\underline{a} \le |a_i(t)| \le \bar{a}, \quad (2b)$$
$$\underline{\delta} \le |\delta_i(t)| \le \bar{\delta}, \quad (2c)$$
$$\underline{r} \le |r_i(t)| \le \bar{r}, \quad (2d)$$
$$\underline{\beta} \le |\beta_i(t)| \le \bar{\beta}. \quad (2e)$$

where $\bar{\cdot}$ and $\underline{\cdot}$ are, respectively, the upper and lower boundaries.

C. Polytopic Representation of CAVs and Road Boundaries

This study represents each CAV$_i$, when $i\in\{1..N\}$ and N is the total number of CAVs, as a rectangular polytope $\tilde{\mathcal{P}}_i$ (i.e., a convex set) that is the intersection area of half-space linear inequalities $\tilde{\mathbf{A}}_i\mathbf{x}\le\tilde{\mathbf{b}}_i$ at the origin, where $\mathbf{x}\in\mathbb{R}^2$ is a Cartesian point. In this paper, all CAVs have the same size which are defined with:

$$\tilde{\mathbf{A}}_i = \begin{bmatrix} 1 & -1 & 0 & 0 \\ 0 & 0 & -1 & 1 \end{bmatrix}^\top, \quad \tilde{\mathbf{b}} = [l/2, l/2, d/2, d/2]^\top. \quad (3)$$

where l and d denote, respectively, the wheelbase and track of CAVs.

As CAV$_i$ moves to a new pose $\mathbf{z}_i(t)=[x_i(t),y_i(t),\theta_i(t)]^T$, the original polytope $\tilde{\mathcal{P}}_i$ of the CAV is transformed to $\mathcal{P}_i$ as follows:

$$\tilde{\mathcal{P}}_i \mapsto \mathcal{P}_i(\mathbf{z}_i;t) : \mathbf{A}_i(\mathbf{z}_i;t)\mathbf{x}(t) \le \mathbf{b}_i(\mathbf{z}_i;t). \quad (4)$$

where:

$$\mathbf{A}_i(\mathbf{z}_i;t) = \tilde{\mathbf{A}}_i\begin{bmatrix} cos\theta_i(t) & sin\theta_i(t) \\ -sin\theta_i(t) & cos\theta_i(t) \end{bmatrix}, \quad (5a)$$

$$\mathbf{b}_i(\mathbf{z}_i;t) = \tilde{\mathbf{b}} + \tilde{\mathbf{A}}_i\begin{bmatrix} cos\theta_i(t) & sin\theta_i(t) \\ -sin\theta_i(t) & cos\theta_i(t) \end{bmatrix}[x_i(t), y_i(t)]^\top. \quad (5b)$$

Fig. 2(b) provides a graphical representation of (4). It is worth noting that the robot pose in (5b) (e.g., $x_i(t), y_i(t)$ and $\theta_i(t)$) do not cause non-convexity as the solver treats them as variables and substitutes values there.

Road boundaries are also modelled as convex polytopic sets $\mathcal{O}_r$, when $r \in \{1..N_r\}$ and N_r is the total number of road boundaries which is 4 for four-legged intersections.

Based on these representations, there is no collision between CAV$_i$ and CAV$_j$ iff $\mathcal{P}_i(\mathbf{z}_i;t) \cap \mathcal{P}_j(\mathbf{z}_j;t) = \emptyset, \forall t \in [t_0, t_f]$. Similarly, CAVs do not collide with road boundaries when the intersection of their sets is always empty, i.e. $\mathcal{P}_i(\mathbf{z}_i;t) \cap \mathcal{O}_r = \emptyset, \forall t \in [t_0, t_f]$.

III. Problem Formulation

This section formulates simultaneous crossing of multiple CAVs through a lane-free and signal-free intersection as an optimal control problem. The formulated OCP minimises the overall crossing time as well as the energy consumption due to acceleration of CAVs whilst avoiding collisions of each vehicle with others and with road boundaries. Rest of the sections provide collision avoidance constraints, initial and terminal conditions and the objective function before presenting the overall OCP formulation.

A. Constraints to Avoid Collisions Between CAVs

To avoid collisions between any CAV$_i$ and CAV$_j$ $\forall i \neq j \in \{1..N\}$, their polytopic sets should not intersect, i.e. $\mathcal{P}_i \cap \mathcal{P}_j = \emptyset$ where $\mathcal{P}_i = \{\mathbf{x} \in \mathbb{R}^2 | \mathbf{A}_i\mathbf{x} \leq \mathbf{b}_i\}$ and $\mathcal{P}_j = \{\mathbf{y} \in \mathbb{R}^2 | \mathbf{A}_j\mathbf{y} \leq \mathbf{b}_j\}$. However, these are non-differentiable conditions and enforcing them as constraints in an OCP will make the problem difficult to be solved by the state-of-the-art gradient-based algorithms. To preserve differentiability and continuity, $\mathcal{P}_i \cap \mathcal{P}_j = \emptyset$ is replaced by the following sufficient condition which has negligible effect on the optimality of the solution for small values of d_{min} [28]:

$$dist(\mathcal{P}_i, \mathcal{P}_j) = \min_{\mathbf{x},\mathbf{y}} \{\|\mathbf{x}-\mathbf{y}\|_2 \mid \mathbf{A}_i\mathbf{x} \leq \mathbf{b}_i,\ \mathbf{A}_j\mathbf{y} \leq \mathbf{b}_j\} \geq d_{min}; \quad \forall i \neq j \in \{1..N\}. \tag{6}$$

where d_{min} is the minimum safe distance between CAVs.

Problem (6) is still non-convex and non-differentiable [28] and the remaining of this subsection is dedicated to reformulate (6) with a smooth and convex sufficient condition.

It is known that the problem of finding the minimum distance between two polytopes $\mathcal{P}_i$ and $\mathcal{P}_j$ (the left hand-side of (6)) is convex [29]. Also, since $\mathcal{P}_j$ is not an empty set, the strong duality holds [28]. This means that the solution of the primal problem of finding $dist(\mathcal{P}_i, \mathcal{P}_j)$ is the same as the one of its dual problem which is as follows:

$$\begin{aligned} \text{dist}(\mathcal{P}_i, \mathcal{P}_j) := \max_{\boldsymbol{\lambda}_{ij}, \boldsymbol{\lambda}_{ij}, \mathbf{s}_{ij}} & -\mathbf{b}_i^\top \boldsymbol{\lambda}_{ij} - \mathbf{b}_j^\top \boldsymbol{\lambda}_{ij} \\ \text{s.t.} \quad & \mathbf{A}_i^\top \boldsymbol{\lambda}_{ij} + \mathbf{s}_{ij} = 0, \mathbf{A}_j^\top \boldsymbol{\lambda}_{ij} - \mathbf{s}_{ij} = 0, \\ & \|\mathbf{s}_{ij}\|_2 \leq 1, -\boldsymbol{\lambda}_{ij} \leq 0, -\boldsymbol{\lambda}_{ij} \leq 0; \\ & \forall i \neq j \in \{1..N\}. \end{aligned} \tag{7}$$

where $\boldsymbol{\lambda}_{ij}$, $\boldsymbol{\lambda}_{ij} \in \mathbb{R}^4$, and $\mathbf{s}_{ij} \in \mathbb{R}^2$ are the dual variables and $\mathbf{A}_i$ and $\mathbf{b}_i$ are as in (5) (the deviation of dual problem (7) from primal problem (6) is shown in [30]). As seen in Fig. 1, $\mathbf{s}_{ij}$ is a separating hyperplane between CAV$_i$ and CAV$_j$ and $\mathbf{s}_{ij} = \mathbf{s}_{ji}$.

Combining (7) with (6), the objective function of (7) subject to its constraints must be greater than or equal to d_{min} in order to avoid collisions. However, (7) can be substituted by $\{\exists \boldsymbol{\lambda}_{ij} \geq 0, \boldsymbol{\lambda}_{ij} \geq 0, \mathbf{s}_{ij} : -\mathbf{b}_i^\top \boldsymbol{\lambda}_{ij} - \mathbf{b}_j^\top \boldsymbol{\lambda}_{ij} \geq d_{cmin}, \mathbf{A}_i^\top \boldsymbol{\lambda}_{ij} + \mathbf{s}_{ij} = 0, \mathbf{A}_j^\top \boldsymbol{\lambda}_{ij} - \mathbf{s}_{ij} = 0, \|\mathbf{s}_{ij}\|_2 \leq 1\}$ because the existence of a feasible solution $\boldsymbol{\lambda}_{ij,feas}$, $\boldsymbol{\lambda}_{ji,feas}$, and $\mathbf{s}_{ij,feas}$ where $-\mathbf{b}_i^\top \boldsymbol{\lambda}_{ij,feas} - \mathbf{b}_j^\top \boldsymbol{\lambda}_{ji,feas} \geq d_{min}$ is a sufficient condition to ensure $dist(\mathcal{P}_i, \mathcal{P}_j) \geq d_{min}$, i.e. to avoid collisions [30]. Also, It is shown in [28] that these sufficient conditions are smooth since the norm operator in $\|\mathbf{s}_{ij}\|_2 \leq 1$ is an Euclidean distance as $\mathbf{s}_{ji} \in \mathbb{R}^2$ and the resulting feasible values of $\mathbf{s}_{ij}$ make a quadratic cone. Moreover, the proposed sufficient conditions replace the nested optimisation problem with feasibility inequality constraints.

B. Constraints to Avoid Collisions With Road Boundaries

Each CAV$_i$ must also avoid all the road boundaries, i.e. $\mathcal{P}_i \cap \mathcal{O}_r = \emptyset$ where $\mathcal{P}_i = \{\mathbf{x} \in \mathbb{R}^2 | \mathbf{A}_i\mathbf{x} \leq \mathbf{b}_i\}$ and $\mathcal{O}_r = \{\mathbf{y} \in \mathbb{R}^2 | \mathbf{A}_r\mathbf{y} \leq \mathbf{b}_r\}$. Similar to section III-A collision avoidance between CAVs, $\mathcal{P}_i \cap \mathcal{O}_r = \emptyset$ is replaced by the following sufficient condition:

$$\text{dist}(\mathcal{P}_i, \mathcal{O}_r) = \min_{\mathbf{x},\mathbf{y}} \{\|\mathbf{x}-\mathbf{y}\|_2 \,|\mathbf{A}_i\mathbf{x} \leq \mathbf{b}_i, \mathbf{A}_r\mathbf{y} \leq \mathbf{b}_r\} \geq d_{rmin}; \quad \forall r \in \{1..N_r\}. \tag{8}$$

where d_{rmin} is the minimum safety distance between CAVs and road boundaries.

The dual problem of (8) is then substituted with the sufficient condition $\{\exists \boldsymbol{\lambda}_{ir} \geq 0, \boldsymbol{\lambda}_{ri} \geq 0, \mathbf{s}_{ir} : -\mathbf{b}_i^\top \boldsymbol{\lambda}_{ir} - \mathbf{b}_r^\top \boldsymbol{\lambda}_{ri} \geq d_{rmin}, \mathbf{A}_i^\top \boldsymbol{\lambda}_{ir} + \mathbf{s}_{ir} = 0, \mathbf{A}_r^\top \boldsymbol{\lambda}_{ri} - \mathbf{s}_{ir} = 0, \|\mathbf{s}_{ir}\|_2 \leq 1\}$ where $\boldsymbol{\lambda}_{ir}, \boldsymbol{\lambda}_{ri}$, and $\mathbf{s}_{ir}$ are the dual variables. $\mathbf{s}_{ir}$ is the separating hyperplane between CAVs and road boundaries (see Fig. 1).

C. Objective Function

CAVs are expected to reach their terminal pose as fast as possible while consume energy (due to acceleration) as little as possible. Therefore, this paper proposes the objective function (9) that minimises the overall crossing time of all CAVs and the error between the current and final pose, as well as the energy consumption due to acceleration of each vehicle:

$$J(\mathbf{z}_1(.), .., \mathbf{z}_N(.)) = \alpha(t_f - t_0)^2 + \int_{t_0}^{t_f} \sum_{i=1}^{N} \left[(\mathbf{z}_i(t) - \mathbf{z}_i(t_f))^\top \mathbf{Q} (\mathbf{z}_i(t) - \mathbf{z}_i(t_f)) + \gamma a_i(t)^2\right] dt\,. \tag{9}$$

where α, $\mathbf{Q}$ and γ are the gain factors related to the crossing time, CAVs' pose and energy consumption (due to acceleration) respectively. The gains are selected based on trail and error to best normalise the cost function. The expression $(t_f - t_0)^2$ minimises the crossing time of all CAVs. The Lagrange term

penalises the error between the current pose $\mathbf{z}_i(t)$ and the final pose $\mathbf{z}_i(t_f)$ as well as the acceleration $a_i(t)^2$ of vehicles. The final pose of CAVs $\mathbf{z}_i(t_f)$ is directly imposed in the objective function and indicates the intended destination of each CAV$_i$.

D. Optimal Control Problem

Lane-free crossing of multiple CAVs through a signal-free intersection is formulated as the following optimal control problem:

$$\{a_i(.), \delta_i(.)\}^* = \tag{10a}$$

$$\arg \min_{t_f, a_i(.), \delta_i(.)} J(\mathbf{z}_1(.), .., \mathbf{z}_N(.)) := (9), \tag{10b}$$

$$\text{s.t.} \quad (1),\ (2), \tag{10c}$$

$$\mathcal{P}_i(t) \cap \mathcal{P}_j(t) = \emptyset;\ \forall i \neq j \in \{1..N\}, \tag{10d}$$

$$\mathcal{P}_i(t) \cap \mathcal{O}_r(t) = \emptyset;\ \forall i \in \{1..N\}, \quad \forall r \in \{1..N_r\},$$

$$\mathbf{z}_i(t_0) = \mathbf{z}_{i,0},\ \forall i \in \{1..N\},\ t \in [t_0, t_f]. \tag{10e}$$

where (10c) refers to the vehicle kinematics and (10d) and (10e) denote, respectively, collision avoidance constraints of each CAV with others and with road boundaries.

As discussed in section III-A and III-B, the non-differentiable and non-convex collision avoidance constraints (10d) and (10e) are substituted by the dual problem of their sufficient conditions (6) and (8), and then (10) is reformulated as the following smooth and continuous problem, which is solvable by the state-of-the-art gradient-based algorithms:

$$\{a_i(.), \delta_i(.)\}^* = \tag{11a}$$

$$\arg \min_{\substack{t_f, a_i(.), \delta_i(.) \\ \boldsymbol{\lambda}_{ij}, \boldsymbol{\lambda}_{ij}, \mathbf{s}_{ij}, \\ \boldsymbol{\lambda}_{ri}, \boldsymbol{\lambda}_{ir}, \mathbf{s}_{ir}}} J(\mathbf{z}_1(.), .., \mathbf{z}_N(.)) := (9),$$

$$\text{s.t.} \quad (1), (2), \tag{11b}$$

$$-\mathbf{b}_i(\mathbf{z}_i(t))^\top \boldsymbol{\lambda}_{ij}(t) - \mathbf{b}_j(\mathbf{z}_j(t))^\top \boldsymbol{\lambda}_{ij}(t) \geq d_{min} \tag{11c}$$

$$\mathbf{A}_i(\mathbf{z}_i(t))^\top \boldsymbol{\lambda}_{ij}(t) + \mathbf{s}_{ij}(t) = 0 \tag{11d}$$

$$\mathbf{A}_j(\mathbf{z}_j(t))^\top \boldsymbol{\lambda}_{ij}(t) - \mathbf{s}_{ij}(t) = 0 \tag{11e}$$

$$-\mathbf{b}_i(\mathbf{z}_i(t))^\top \boldsymbol{\lambda}_{ir}(t) - \mathbf{b}_r^\top \boldsymbol{\lambda}_{ri}(t) \geq d_{rmin} \tag{11f}$$

$$\mathbf{A}_i(\mathbf{z}_i(t))^\top \boldsymbol{\lambda}_{ir}(t) + \mathbf{s}_{ir}(t) = 0 \tag{11g}$$

$$\mathbf{A}_r^\top \boldsymbol{\lambda}_{ri}(t) - \mathbf{s}_{ir}(t) = 0 \tag{11h}$$

$$\boldsymbol{\lambda}_{ij}(t),\ \boldsymbol{\lambda}_{ij}(t),\ \boldsymbol{\lambda}_{ir}(t),\ \boldsymbol{\lambda}_{ri}(t) \geq 0, \tag{11i}$$

$$\|\mathbf{s}_{ij}(t)\|_2 \leq 1,\ \|\mathbf{s}_{ir}(t)\|_2 \leq 1, \tag{11j}$$

$$\mathbf{z}_i(t_0) = \mathbf{z}_{i,0}, \tag{11k}$$

$$\forall i \neq j \in \{1..N\}, \forall r \in \{1..N_r\}.$$

where $\mathbf{A}_i$ and $\mathbf{b}_i$ are functions of each CAV's pose $\mathbf{z}_i(t)$, and present CAV$_i$ polytope at each time step t. Problem (11) is solved at time t_0 for N CAVs until the terminal time t_f. The solution to this problem is optimal trajectories of the control signals $a_i(.)^*$ and $\delta_i(.)^*$ of each CAV$_i$ for each $t \in [t_0, t_f]$, as well as a terminal time t_f. CAVs follow their calculated trajectories to arrive their final destinations at the terminal time t_f.

The initial pose $\mathbf{z}_i(t_0)$, i.e. initial position, heading angle and initial speed of all CAV$_i$ $\forall i \in \{1..N\}$ within the control zone are known. The remaining of the states and the initial inputs to the CAVs are also assumed as zero. These initial conditions at $t = t_0$ are feasible solutions of the OCP.

TABLE II
MAIN PARAMETERS OF THE MODEL

Parameter(s)	Description	Value(s)
m (kg)	mass of each CAV	1204
d_{min} (m)	minimum distance between CAVs	0.1
d_{rmin} (m)	minimum distance between CAVs and road boundaries	0.1
d (-)	number of collocation points	5
N_p (-)	number of control intervals	30
$\bar{V}$ (m/s)	upper bound on V_i	25
$\underline{V}$ (m/s)	lower bound on V_i	0
$\bar{\delta}$ = -$\underline{\delta}$ (rad)	bounds on $\lvert\delta_i\rvert$	0.67
$\bar{a} = -\underline{a}$ (m/s^2)	bounds on $\lvert a_i\rvert$	3
$\bar{r}$ = -$\underline{r}$ (rad/s)	bounds on $\lvert r_i\rvert$	0.7
$\bar{\beta}$ = -$\underline{\beta}$ (rad)	bounds on $\lvert\beta_i\rvert$	0.5
$V_i(t_0)$ $\forall i \in \{1..N\}$ (m/s)	initial speed of CAVs	10

IV. RESULTS AND DISCUSSION

In this section, performance of the proposed algorithm is compared against two state-of-the-art benchmarks in terms of crossing time, energy consumption due to acceleration and passenger comfort. For doing this, this study employs the intersection scenario proposed in [14], which is named test scenario one hereafter. The first benchmark is a conflict-point-reservation approach presented in [14], where each CAV calculates its own trajectory by jointly minimising the travelling time and energy consumption (due to acceleration). The calculated reservation times for each conflict point are then shared with other vehicles through a centralised coordinator. Vehicles entering the intersection later read these reserved times and treat them as additional collision avoidance constraints when they plan their own trajectory. The second benchmark is a lane-free method proposed in [16] where CAVs can freely use all the space of the junction, as long as there is no collision. The proposed algorithm in [16] calculates the control inputs for a relatively large given value of crossing time.

The algorithms are compared within test scenario one in terms of crossing time, average and standard deviation of speed and energy consumption (due to acceleration) for different number of CAVs between 2 to 12. The initial and terminal pose of CAVs are chosen randomly and there exists at least one CAV performing a left-turn manoeuvre in each test. Table II summarises values of the parameters used in the proposed and benchmark algorithms. The vehicle parameters and boundaries are typical values for a passenger car. It is assumed that the vehicles only move

forward. The control intervals N_p and number of collocation points d are tuned to get the best performance with the minimum computational time.

Furthermore, the performance of the proposed algorithm is analysed for two more complex scenarios, which is named test scenario two and test scenario three hereafter. These two scenarios involve up to 21 CAVs, and allow any travelling direction by CAVs (e.g., right, straight and left).

CasADi [31] and IPOPT [32] are used to solve the formulated nonlinear OCP (11). CasADi allows to discretise a minimum-time OCP using the collocation method and construct an equivalent nonlinear programming (NLP) with the final time as an augmented decision variable [33]. The final time divided by a given number of control intervals N_p appears as the sampling time to discretise (1). The resulting sparse NLP is then solved by IPOPT (that implements the interior-point method) which is shown to be superior to solve sparse problems [34]. To improve the computation time, IPOPT is linked to IntelÂ oneAPI Math Kernel Library (oneMKL, https://software.intel.com), which includes high-performance implementation of the *MA27* linear solver. All the results are calculated with MATLAB running on a Linux Ubuntu 20.04.0 LTS server with a 3.7 GHz IntelÂ Core i7 and 32 GB of memory.

A. Crossing Time

This section compares the minimum crossing time of CAVs that can be achieved by the developed and benchmark algorithms. The acceleration gain γ in (9) is set to zero to calculate the minimum-time travelling trajectories of CAVs. In other words, the energy consumption due to acceleration is not considered and CAVs only try to reach destinations as fast as possible, which makes the problem single objective.

Table III compares crossing time of CAVs when they are controlled by the developed and benchmark algorithms during test scenario one. The table also summarises energy consumption due to acceleration, the travelled distance and average and standard deviation of speed of CAVs. It is worth noting that the crossing time is defined as the time required for all the under-control CAVs to cross the intersection and arrive to their destinations. Also, the travelled distance and energy consumption are calculated for all the crossing CAVs.

As seen in Table III, crossing time of CAVs when they are controlled by the proposed algorithm is, respectively, up to 65% (for 12 CAVs and in average 52% for all number of crossing CAVs), and 54% less than the case where CAVs are controlled by the reservation-based approach in [14] and the lane-free method in [16]. This is, of course, in cost of higher energy consumption (due to acceleration), as the objective function of the proposed algorithm only considers minimisation of travelling time. The next subsection provides a detail analysis on energy consumption due to acceleration of different approaches, and shows that the proposed algorithm can still achieve significant improvement in crossing time while consuming the same amount of energy (due to acceleration) as the reservation-based method in [14].

It is also shown in Table III that, unlike the reservation-based strategy, the resulting crossing time of the proposed algorithm does not change regardless of number of crossing CAVs. There is a similar trend for the average and standard deviation of speed of CAVs when they are controlled by the developed strategy. Also, it is evident from Table III that the standard deviation of the speed of crossing CAVs when they are controlled by the proposed algorithm is mostly less than the case when they are controlled by the reservation based strategy in [14]. Apparently, the smaller value of standard deviation of speed indicates a less diverge set of speeds (i.e., smoother travel) for the crossing CAVs.

Table IV shows crossing time, average and standard deviation of speed and travelled distance for different number of CAVs when they are controlled by the proposed strategy in test scenario

TABLE III
PERFORMANCE OF THE PROPOSED LANE-FREE METHOD FOR TEST SCENARIO ONE AS COMPARED TO THE RESERVATION-BASED METHOD IN [14] AND THE LANE-FREE METHOD IN [16].

Number of CAVs →	**2**	**4**	**6**	**8**	**10**	**12**
The proposed algorithm						
Crossing time (s)	4.56	4.57	4.57	4.57	4.57	4.57
Average speed (m/s)	15.2	15.8	15.6	15.1	15.4	15.5
Standard deviation of speed	3.5	3.8	3.7	3.4	3.6	3.7
Energy consumption due to acceleration (kWh)	0.1	0.23	0.33	0.39	0.52	0.65
Travelled distance (m)	130	270	400	518	658	799
Reservation-based [14]						
Crossing time (s)	6.29	6.29	12.50	12.93	12.92	12.92
Average speed (m/s)	12.7	13.5	11.3	9.9	10.6	11.1
Standard deviation of speed	2.3	2.5	4.4	4.4	4.6	4.6
Energy consumption due to acceleration (kWh)	0.03	0.07	0.05	0.04	0.06	0.07
Travelled distance (m)	134	265	406	507	630	750
Lane-free [16]						
Crossing time (s)	10	10	10	10	10	10
Average speed (m/s)	10.1	10.0	10.0	10.0	10.1	10.0
Standard deviation of speed	0.1	0.1	0.1	0.2	0.2	0.2
Energy consumption due to acceleration (kWh)	0.001	0.001	0.001	0.003	0.006	0.006
Travelled distance (m)	195	387	577	773	973	1160

TABLE IV
SIMULATION RESULTS OF THE PROPOSED ALGORITHM IN TEST SCENARIO TWO AND THREE FOR DIFFERENT NUMBER OF CAVS

Number of CAVs →	**3**	**6**	**9**	**12**	**15**	**18**	**21**
Test scenario two							
Crossing time (s)	4.57	4.57	4.57	4.56	4.57	4.58	4.57
Average speed (m/s)	13.2	14.5	14.5	14.2	14.1	13.8	13.6
Standard deviation of speed	3.9	4.0	3.8	3.9	4.1	4.2	4.1
Energy consumption due to acceleration (kWh)	0.11	0.27	0.4	0.5	0.64	0.7	0.8
Travelled distance (m)	170	373	561	730	910	1067	1224
Test scenario three							
Crossing time (s)	4.44	4.55	4.55	4.57	4.55	4.55	4.57
Average speed (m/s)	13.1	13.4	13.4	13.0	13.6	13.0	13.0
Standard deviation of speed	2.4	2.9	2.3	2.8	3.1	3.3	3.4
Energy consumption due to acceleration (kWh)	0.08	0.18	0.26	0.34	0.50	0.55	0.65
Travelled distance (m)	165	344	516	675	874	1002	1171

two and three. As shown, crossing time of CAVs in both the test scenario two and three is the same as the one in test scenario one, and again does not change regardless of the number of CAVs. This determines that the crossing time of lane-free intersections is not sensitive to the type of scenario and number of CAVs. This is an interesting outcome that shows in lane-free intersections, the crossing time of CAVs is limited by the layout of the junction rather than by the number of passing CAVs, as in traditional signalised intersections.

In fact, crossing time of CAVs cannot be theoretically smaller than the travelling time of the CAV that drives the longest distance with its maximum permissible acceleration. In other words, the minimum crossing time is dominated by the CAV that is furthest from the intersection and those closer CAVs to the junction do not change the crossing time. In all three scenarios, the initial speed of CAVs $V(t_0)$ is 10 (m/s), the maximum travelling distance (e.g, the travelling distance of the CAV that is furthest away from the intersection) $\triangle x$ is 70 (m) and the maximum acceleration $\bar{a}$ is 3 (m/s^2), and hence the theoretical lower bound of crossing time is 4.27 (s) calculated by the Newton's law $\triangle x = \frac{1}{2}\bar{a} \times t^2 + V(t_0) \times t$. The results in Table III and IV show that the proposed algorithm finds a very close value to this theoretical boundary regardless of type of scenario and number of crossing CAVs. In fact, the resulting crossing time can be as close as desired to the theoretical bound in cost of deviation of final point from the desired destination point.

Fig. 3 shows the calculated optimal vehicle motion and speed trajectory for the proposed algorithm in all three test scenarios with the maximum number of CAVs (i.e., 12 for test scenario one and 21 for the test scenario two and three). As shown in Fig. 3 b, 3 d and 3 f the proposed strategy increases and decreases the speed of CAVs linearly to avoid collisions. The slope of variation (i.e., acceleration and deceleration) is 3 (m/s^2) indicating that it is a bang-bang strategy. Moreover, the motion trajectory Figs. 3 a, 3 c and 3 e illustrate that CAVs move and use opposite lanes freely while avoiding road boundaries. The results are also visualised by a provided video on.[1]

It must be noted that the possibility of collision between two consecutive control intervals is zero because the chosen sampling time is 0.152 (s) which is less than the threshold. The threshold value is calculated based on the minimum sampling time required for a CAV to travel a distance of one length $(2.6\,m)$ + one width $(1.56\,m)$ of a vehicle with its maximum permissible speed $\frac{2.6+1.56}{25} = 0.166$ (s). In other words, for the obtained minimum crossing time of 4.57 s, mid-point collisions are infeasible for any number of control intervals N_p greater than or equal to $\frac{4.57}{0.166} \approx 28$. This paper chooses a value of 30 for the number of control intervals which exceeds the threshold with a low computational time.

Fig. 4 depicts computational time of the proposed algorithm for different number of CAVs in test scenario two. The computation time of each number of CAV is the average of 10 times of running the scenario. The standard deviations of all the tests are less than 0.5% which is negligible and are not shown. Fig. 4 shows that the computational complexity of the proposed algorithm is of the order of $O(e^{0.13\,N})$ in terms of number of CAVs N. The computational time of (11) can be reduced by decentralising the proposed strategy, as a future work. Moreover, model-predictive control (MPC) will be used for real-time implementation of (11). MPC solves the OCP with a shorter prediction horizon and hence reduces the computation time. To compensate the resulting uncertainty, MPC takes into account a feedback from the system and resolves the problem over a receding horizon.

[1]https://www.youtube.com/watch?v=S2GiGPQAfow

B. Energy Consumption

Fig 5 a illustrates the total energy consumption due to acceleration of CAVs when the vehicles are controlled by the proposed and benchmark strategies in test scenario one. The figure also shows the total energy consumption of CAVs being controlled by the proposed strategy in test scenario two and three. The depicted graphs only consider the energy consumption due to acceleration which is calculated as follows:

$$E_i = m \int_{t_0}^{t_f} a_i(t) v_i(t) dt$$

where E_i is the energy consumed by each CAV$_i$.

As seen in Fig. 5 a, the lane-free method proposed in [16] consumes the least energy, in cost of fixing the crossing time to an unnecessarily large value (i.e., 10 s). The proposed algorithm in this paper, in contrast, consumes more energy than both the benchmark strategies because it is optimised for minimisation of crossing time, as explained in section IV-A.

Moreover, the resulting energy consumption (due to acceleration) of the proposed strategy linearly increases with respect to the number of crossing CAVs in all the three test scenarios. It can also be observed that CAVs consume more energy in test scenario one than in test scenario two and three because of a longer travelling distance due to diversity of destination of CAVs. The travelled distance values of test scenario one is provided in Table III and for test scenario two and three in Table IV.

Fig. 5 b, on the other hand, compares the algorithms in terms of the energy consumption by each vehicle when travels one kilometer. As seen, all the strategies tend to consume less energy per vehicle per kilometer with an increase in the number of CAVs. This is due to the fact that the number of obstacles drops by reducing the number of crossing CAVs, and hence vehicles can accelerate and pass through faster in test scenario one.

To nullify energy consumption as one of the objectives, and only compare the crossing time of CAVs when they are controlled by the proposed strategy and the reservation-based one in [14], the acceleration gain γ in (9) is tuned such that energy consumption due to acceleration of CAVs in both cases becomes the same. Table V shows the resulting performance of the proposed algorithm. As compared to the results of the reservation-based method in Table III, the proposed algorithm reduces the crossing time up to 52% (average of 40%) when consumes the same amount of energy. Moreover, whilst the average speed of CAVs is almost similar for both the strategies, the

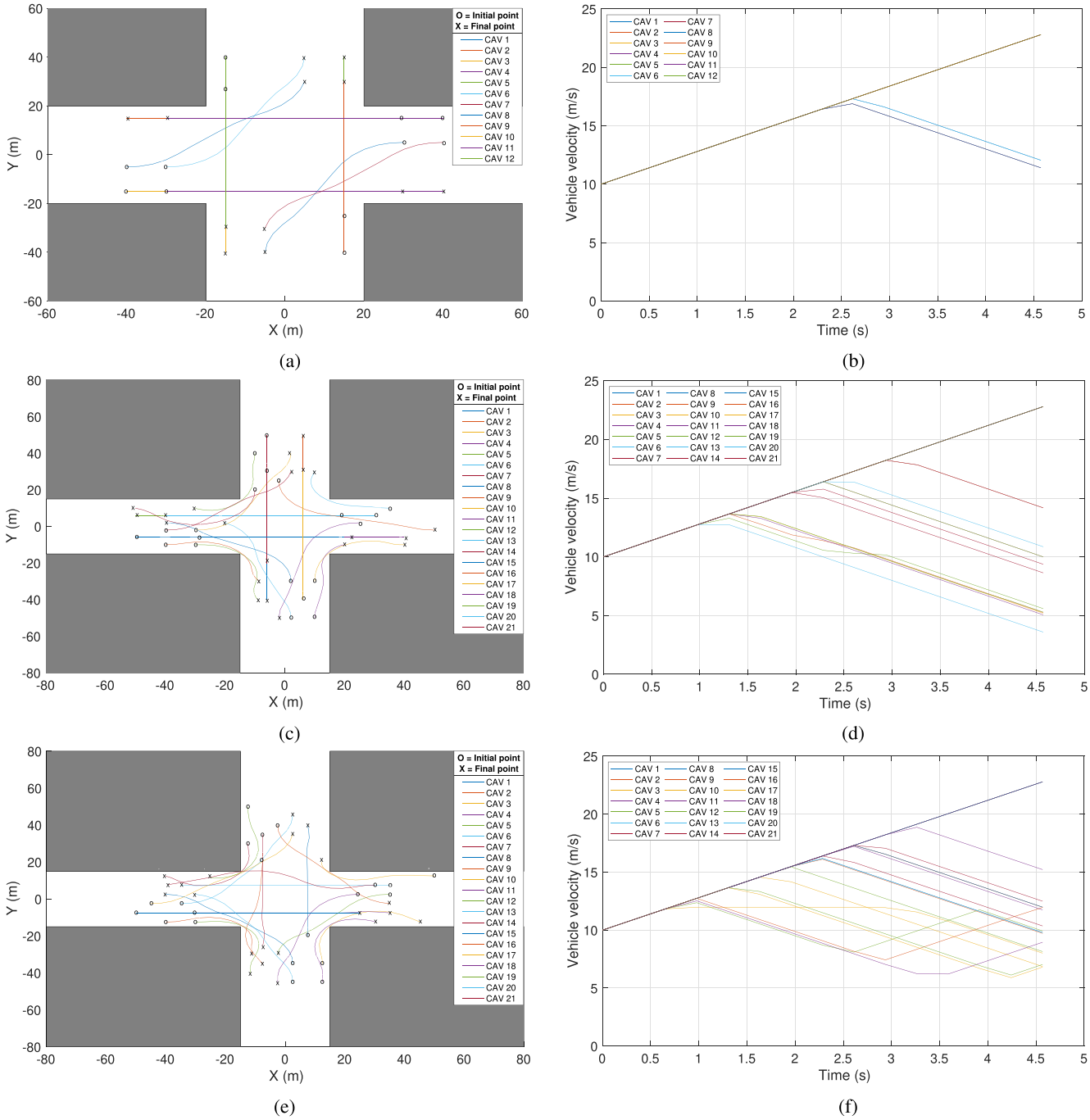

Fig. 3. The calculated optimal trajectories of motion and speed using the proposed algorithm in test scenario one, two, and three for 12, 21, and 21 CAVs respectively. (a) Test scenario one's motion trajectory. (b) Test scenario one's speed trajectory. (c) Test scenario two's motion trajectory. (d) Test scenario two's speed trajectory. (e) Test scenario three's motion trajectory. (f) Test scenario three's speed trajectory.

standard deviation of speed of CAVs controlled by the proposed algorithm is much lower. This indicates that CAVs controlled by the proposed algorithm travel with similar speed, whilst some of the CAVs being controlled by the reservation-based method travel with a much higher or lower speed than the others.

Fig. 6 depicts that the proposed algorithm finds the Pareto front of all the crossing solutions of 12 CAVs for different values of acceleration gain γ. As seen, the proposed strategy can achieve shorter crossing time than both the reservation-based method [14] and lane-free method [16] while consuming the same amount of energy.

Furthermore, Fig. 6 shows that the minimum crossing time of the proposed strategy in all three scenarios is 4.57 s. This indicates that the minimum crossing time of the proposed algorithm is independent of the type of scenario and confirms the data provided in Tables III and IV. However, it can be seen from Fig. 6 that the crossing time is slightly dependent to the type of scenario when CAVs consume minimal energy. This can be due

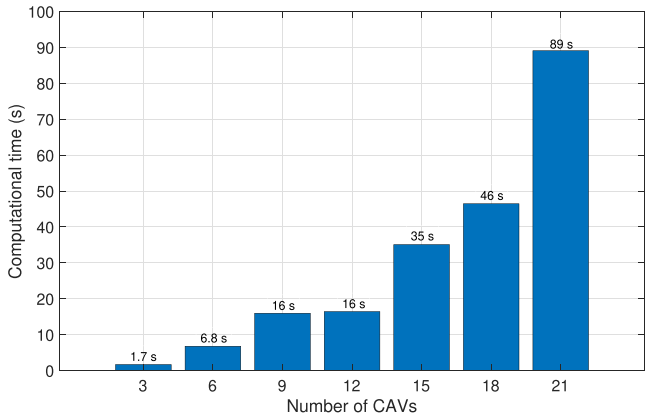

Fig. 4. The average computational time of 10 runs of the proposed strategy for different number of CAVs with test scenario two. The standard deviation of the 10 runs for each number of CAVs is less than 0.5%.

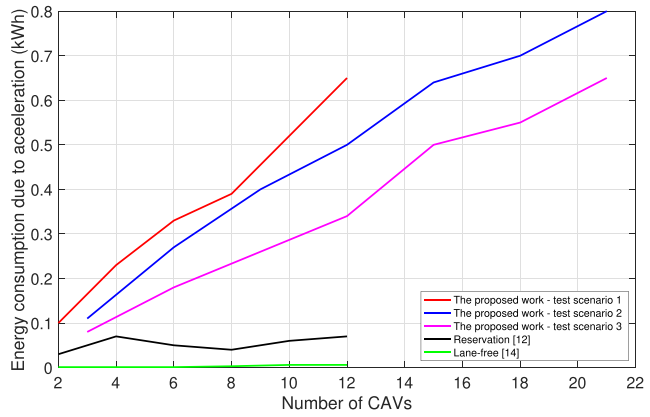

(a)

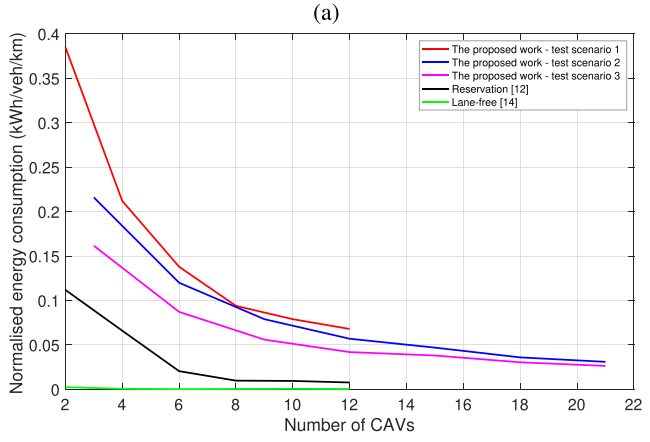

(b)

Fig. 5. Comparison of (a) total energy consumption due to acceleration (b) energy due to acceleration consumed per vehicle per kilometer for different number of vehicles.

to CAVs finding trajectories that tend to be energy efficient but are longer to travel.

It is worth noting that the minimum crossing time of CAVs can be as close as possible to its theoretical lower bound however at the cost of deviation from the final point.

TABLE V
PERFORMANCE OF THE PROPOSED LANE-FREE METHOD IN TEST SCENARIO ONE WHEN THE ENERGY CONSUMPTION IS THE SAME AS THE RESERVATION-BASED STRATEGY IN [14].

Number of CAVs →	**2**	**4**	**6**	**8**	**10**	**12**
Crossing time (s)	5.23	5.30	5.97	6.18	6.24	6.27
Average speed (m/s)	13.3	13.6	12.0	11.3	11.3	11.4
Standard deviation of speeds	1.7	1.7	1.1	1.0	1.0	1.0
Energy consumption due to acceleration (kWh)	0.03	0.07	0.05	0.04	0.06	0.07
Travelled distance (m)	131	270	401	521	661	801

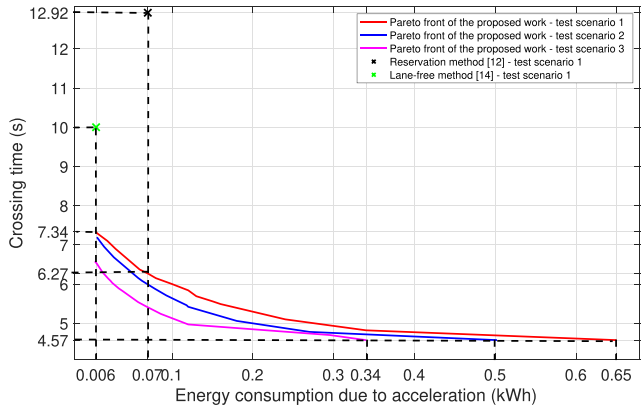

Fig. 6. Energy due acceleration vs crossing time (Pareto front) of 12 CAVs controlled by the proposed strategy as compared to the results by the reservation method in [14] and the lane-free method in [16].

C. Passenger Comfort

Fig. 7 compares the calculated optimal vehicle speed, longitudinal and lateral acceleration (or deceleration) trajectories by the proposed algorithm with the results of the reservation-based method in [14] for 12 CAVs in test scenario one, when the energy consumption due to acceleration is the same ($\beta << 1$).

Fig. 7 a as compared to Fig. 7 b shows that the vehicles travel within a much narrower range of speed and hence the passengers experience similar feeling of speed when CAVs are controlled by the proposed algorithm as opposed to the reservation-based method in [14].

Moreover, as shown in Fig. 7 c, the maximum deceleration of CAVs when they are controlled by the proposed strategy is $1.4\,(m/s^2)$ which is much less than the maximum permissible value of $3\,(m/s^2)$. The acceleration of all CAVs also converges to zero at their destinations. Fig. 7 c, on the other hand, shows that some of the CAVs controlled by the reservation-based algorithm in [14] decelerate with the maximum permissible value, which is not converged to zero.

The maximum jerk of both algorithms is around $0.6\ m/s^3$, however, whilst jerks of CAVs controlled by the proposed strategy converge to zero, the passengers feel an uncomfortably constant jerk during the crossing time when CAVs are controlled by the reservation-based method in [14].

In contrast, Figs. 7 d and 7 e illustrate that passengers of the cornering vehicles, i.e., CAV_i $i \in \{1, 6, 7, 8\}$, experience sharper variation of lateral acceleration when the vehicles are

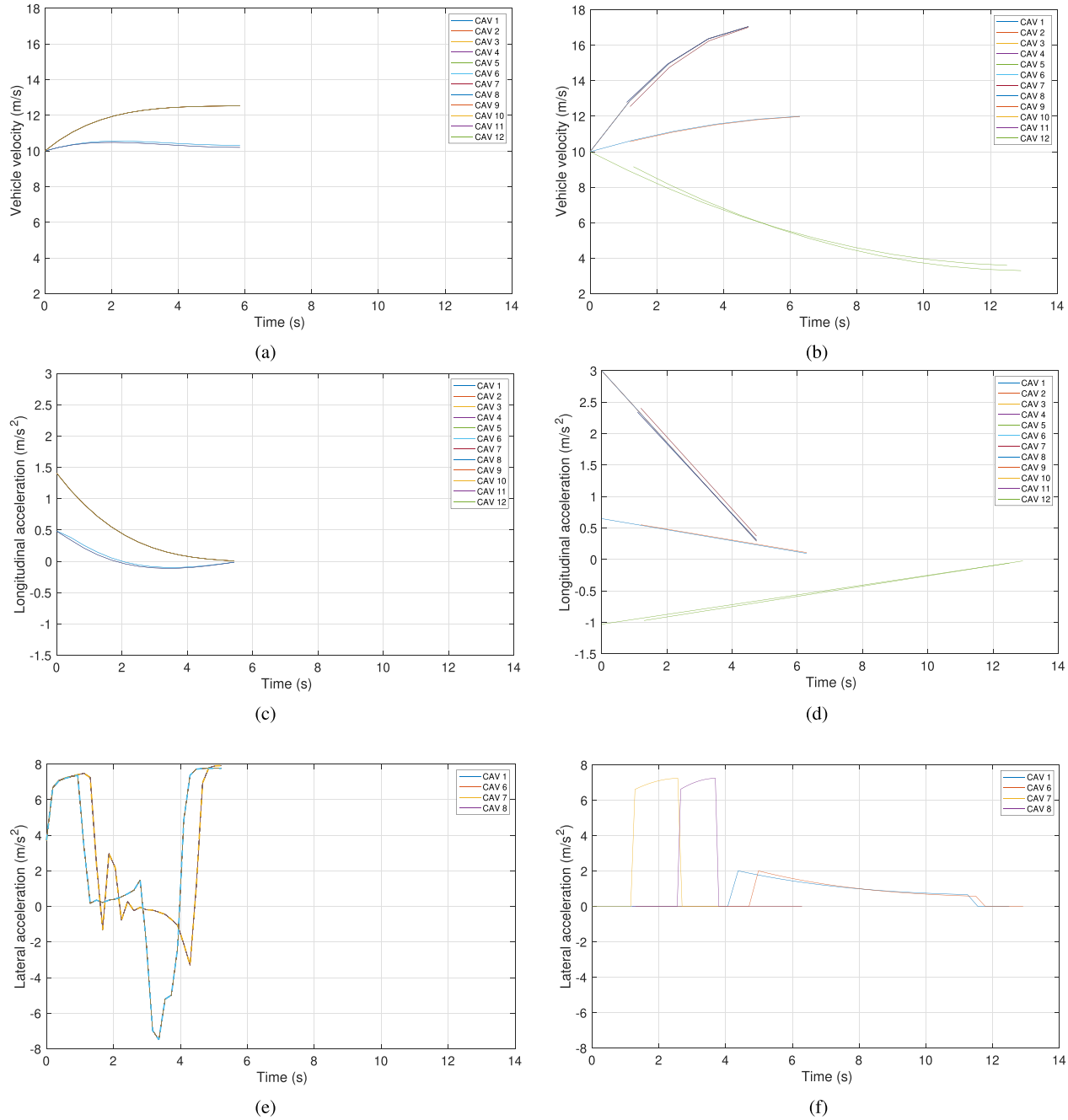

Fig. 7. The calculated optimal trajectories of speed and acceleration using the proposed algorithm and reservation-based method [14] in test scenario one for 12 CAVs, when energy consumption is the same. (a) The proposed algorithm's speed trajectory. (b) The reservation-based method [14] speed trajectory. (c) The proposed algorithm's longitudinal acceleration trajectory. (d) The reservation-based method [14] longitudinal acceleration trajectory. (e) The proposed algorithm's lateral acceleration trajectory. (f) The reservation-based method [14] lateral acceleration trajectory.

controlled by the proposed algorithm than the algorithm in [14], even though the maximum values are almost similar. This is due to the fact that the proposed algorithm generates higher lateral acceleration to achieve shorter travelling time.

V. Conclusion

This study formulates the lane-free crossing of CAVs through intersections as an optimal control problem that minimises the overall crossing time and energy consumption due to acceleration of CAVs while avoiding obstacles. The proposed formulation employs dual problem theory to substitute the non-differentiable and non-convex constraints of collision avoidance with the dual problem of a corresponding sufficient condition.

The resulting smoothed OCP is then solved by CasADi to generate a strategy for safely cross of multiple CAVs through a junction within the minimum time. It is shown that the lane-free crossing is capable of significantly reducing the crossing time

as compared to the state-of-the-art reservation-based strategy, whilst consuming similar energy.

The presented results confirm that the proposed strategy finds the minimum crossing time of CAVs which is very close to its theoretical limit. Also, it shows that the calculated time only relies on the layout of intersection and is independent of the number of crossing CAVs or their manoeuvres. This makes the results of the proposed algorithm a suitable benchmark to evaluate the performance of other control strategies of the CAVs crossing intersections.

Computational complexity of solving the proposed OCP is of the order of $O(e^{0.13\,N})$, where N is the number of CAVs passing through the intersection. As a future work, the authors plan to realise the proposed strategy as a decentralised algorithm over a receding horizon that can be applied to the real-time applications.

REFERENCES

[1] U.S. Department of Trasnportation, "State transportation statistics," 2012. [Online]. Available: https://www.bts.gov/editorial-type/legacy-publication?page=152

[2] J. Rios-Torres and A. A. Malikopoulos, "A survey on the coordination of connected and automated vehicles at intersections and merging at highway on-ramps," *IEEE Trans. Intell. Transp. Syst.*, vol. 18, no. 5, pp. 1066–1077, May 2017.

[3] Y. Zhang, A. A. Malikopoulos, and C. G. Cassandras, "Decentralized optimal control for connected automated vehicles at intersections including left and right turns," in *Proc. IEEE 56th Annu. Conf. Decis. Control*, 2017, pp. 4428–4433.

[4] P. Tallapragada and J. Cortés, "Hierarchical-distributed optimized coordination of intersection traffic," *IEEE Trans. Intell. Transp. Syst.*, vol. 21, no. 5, pp. 2100–2113, May 2020.

[5] B. Xu et al., "Distributed conflict-free cooperation for multiple connected vehicles at unsignalized intersections," *Transp. Res. Part C: Emerg. Technol.*, vol. 93, pp. 322–334, 2018.

[6] M. Di Vaio, P. Falcone, R. Hult, A. Petrillo, A. Salvi, and S. Santini, "Design and experimental validation of a distributed interaction protocol for connected autonomous vehicles at a road intersection," *IEEE Trans. Veh. Technol.*, vol. 68, no. 10, pp. 9451–9465, Oct. 2019.

[7] L. Makarem and D. Gillet, "Fluent coordination of autonomous vehicles at intersections," in *Proc. IEEE Int. Conf. Syst., Man, Cybern.*, 2012, pp. 2557–2562.

[8] A. Mirheli, L. Hajibabai, and A. Hajbabaie, "Development of a signal-head-free intersection control logic in a fully connected and autonomous vehicle environment," *Transp. Res. Part C, Emerg. Technol.*, vol. 92, pp. 412–425, 2018.

[9] A. Mirheli, M. Tajalli, L. Hajibabai, and A. Hajbabaie, "A consensus-based distributed trajectory control in a signal-free intersection," *Transp. Res. Part C, Emerg. Technol.*, vol. 100, pp. 161–176, 2019.

[10] H. Xu, C. G. Cassandras, L. Li, and Y. Zhang, "Comparison of cooperative driving strategies for CAVs at signal-free intersections," *IEEE Trans. Intell. Transp. Syst.*, vol. 23, no. 7, pp. 7614–7627, Jul. 2022.

[11] M. Cai et al., "Multi-lane unsignalized intersection cooperation with flexible lane direction based on multi-vehicle formation control," *IEEE Trans. Veh. Technol.*, vol. 71, no. 6, pp. 5787–5798, Jun. 2022.

[12] Z. He, L. Zheng, L. Lu, and W. Guan, "Erasing lane changes from roads: A design of future road intersections," *IEEE Trans. Intell. Veh.*, vol. 3, no. 2, pp. 173–184, Jun. 2018.

[13] X. Pan, B. Chen, S. A. Evangelou, and S. Timotheou, "Optimal motion control for connected and automated electric vehicles at signal-free intersections," in *Proc. IEEE 59th Conf. Decis. Control*, 2020, pp. 2831–2836.

[14] A. A. Malikopoulos, L. Beaver, and I. V. Chremos, "Optimal time trajectory and coordination for connected and automated vehicles," *Automatica*, vol. 125, 2021, Art. no. 109469.

[15] B. Li, Y. Zhang, Y. Zhang, N. Jia, and Y. Ge, "Near-optimal online motion planning of connected and automated vehicles at a signal-free and lane-free intersection," in *Proc. IEEE Intell. Veh. Symp.*, 2018, pp. 1432–1437.

[16] B. Li, Y. Zhang, N. Jia, and X. Peng, "Autonomous intersection management over continuous space: A microscopic and precise solution via computational optimal control," *IFAC-PapersOnLine*, vol. 53, no. 2, pp. 17071–17076, 2020.

[17] C. Liu, C.-W. Lin, S. Shiraishi, and M. Tomizuka, "Distributed conflict resolution for connected autonomous vehicles," *IEEE Trans. Intell. Veh.*, vol. 3, no. 1, pp. 18–29, Mar. 2018.

[18] R. Hult, M. Zanon, S. Gros, and P. Falcone, "Optimal coordination of automated vehicles at intersections with turns," in *Proc. 18th Eur. Control Conf.*, 2019, pp. 225–230.

[19] R. Hult, M. Zanon, S. Gros, H. Wymeersch, and P. Falcone, "Optimisation-based coordination of connected, automated vehicles at intersections," *Veh. Syst. Dyn.*, vol. 58, no. 5, pp. 726–747, 2020.

[20] A. Katriniok, P. Kleibaum, and M. Joševski, "Distributed model predictive control for intersection automation using a parallelized optimization approach," *IFAC-PapersOnLine*, vol. 50, no. 1, pp. 5940–5946, 2017.

[21] M. Kloock, P. Scheffe, S. Marquardt, J. Maczijewski, B. Alrifaee, and S. Kowalewski, "Distributed model predictive intersection control of multiple vehicles," in *Proc. IEEE Intell. Transp. Syst. Conf.*, 2019, pp. 1735–1740.

[22] A. A. Malikopoulos, C. G. Cassandras, and Y. J. Zhang, "A decentralized energy-optimal control framework for connected automated vehicles at signal-free intersections," *Automatica*, vol. 93, pp. 244–256, 2018.

[23] Y. Bian, S. E. Li, W. Ren, J. Wang, K. Li, and H. X. Liu, "Cooperation of multiple connected vehicles at unsignalized intersections: Distributed observation, optimization, and control," *IEEE Trans. Ind. Electron.*, vol. 67, no. 12, pp. 10744–10754, Dec. 2020.

[24] D. Elliott, W. Keen, and L. Miao, "Recent advances in connected and automated vehicles," *J. Traffic Transp. Eng. (English Ed.)*, vol. 6, no. 2, pp. 109–131, 2019.

[25] M. Papageorgiou, K.-S. Mountakis, I. Karafyllis, I. Papamichail, and Y. Wang, "Lane-free artificial-fluid concept for vehicular traffic," *Proc. IEEE*, vol. 109, no. 2, pp. 114–121, Feb. 2021.

[26] K. Chavoshi and A. Kouvelas, "Distributed control for laneless and directionless movement of connected and automated vehicles," in *Proc. 21st Swiss Transport Res. Conf.*, Ascona, Switzerland, Sep. 12–14, 2021.

[27] W. Milliken and D. Milliken, Race car vehicle dynamics, ser. premiere series. SAE International, 1995. [Online]. Available: https://books.google.co.uk/books?id=opgHfQzlnLEC

[28] X. Zhang, A. Liniger, and F. Borrelli, "Optimization-based collision avoidance," *IEEE Trans. Control Syst. Technol.*, vol. 29, no. 3, pp. 972–983, May 2021.

[29] S. Boyd and L. Vandenberghe, *Convex Optimization*. Cambridge, U.K.: Cambridge Univ. Press, 2004.

[30] R. Firoozi, L. Ferranti, X. Zhang, S. Nejadnik, and F. Borrelli, "A distributed multi-robot coordination algorithm for navigation in tight environments," 2020, *arXiv:2006.11492*.

[31] J. A. E. Andersson, J. Gillis, G. Horn, J. B. Rawlings, and M. Diehl, "CasADi–A software framework for nonlinear optimization and optimal control," *Math. Program. Comput.*, vol. 11, no. 1, pp. 1–36, 2019.

[32] A. Wächter and L. T. Biegler, "On the implementation of an interior-point filter line-search algorithm for large-scale nonlinear programming," *Math. Program.*, vol. 106, no. 1, pp. 25–57, 2006.

[33] C. Rösmann, A. Makarow, and T. Bertram, "Time-optimal control with direct collocation and variable discretization," 2020*arXiv:2005.12136*, .

[34] R. Bartlett, A. Wachter, and L. Biegler, "Active set vs. interior point strategies for model predictive control," in *Proc. Amer. Control Conf.*, 2000, pp. 4229–4233.

Mahdi Amouzadi received the B.Eng. degree in electrical and electronic engineering in 2019 from the University of Sussex, Brighton, U.K., where he is currently working toward the Ph.D. degree with the Smart Vehicles Control Laboratory, Department of Engineering and Informatics. His research interests inlcude the intersection of control and optimization of connected autonomous vehicles. He is focused on designing safe and efficient path planning algorithms for congested areas, such as intersections.

Mobolaji Olawumi Orisatoki received the B.Sc. degree in computer science from the University of Greenwich, London, U.K., in 2006, the M.Sc. degree from the Royal Holloway, University of London, London, U.K., in 2012, and PGCE from the Institute of Education-University College London, London, U.K., in 2013. He is currently working toward the Ph.D. degree with the Smart Vehicles Control Laboratory, Department of Engineering and Design, University of Sussex, Brighton, U.K. He has taught in different colleges across South and East London. His research interests include system optimization and control, system dynamics, multi-agent systems, information entropy and mapping. He is focused on designing an algorithm to map of a non-convex area, maximizing information with travelling distance.

Arash M. Dizqah (Member, IEEE) received the M.Eng. degree in electrical engineering from the Sharif University of Technology, Tehran, Iran, in 1998, the M.Sc. degree in electrical engineering from the K.N. Toosi Universitie of Technology, Tehran, Iran, in 2001, and the Ph.D. degree in control engineering from Northumbria University, London, U.K., in 2014. He is currently a Senior Lecturer in mechanical engineering with the University of Sussex, Brighton, U.K. His research focuses on control and optimisation with applications in vehicles and robotics. He is particularly interested in the real-time implementation of distributed nonlinear optimisation-based controllers for connected and autonomous vehicles and for informative path planning with a team of robots. He is the Director of the Smart Vehicles Control Laboratory, focusing on advanced control strategies for connected and autonomous vehicles, swarm robotics and energy management strategies. He was a Research Fellow with the University of Surrey, Guildford, U.K.